ResearchGate

See discussions, stats, and author profiles for this publication at: https://www.researchgate.net/publication/263954060

Novel Optimized Process for Utilization of CaO-Based Sorbent for Capturing CO2 and SO2 Sequentially

ARTICLE *in* ENERGY & FUELS · AUGUST 2012

Impact Factor: 2.79 · DOI: 10.1021/ef300487q

CITATIONS
8

READS
35

6 AUTHORS, INCLUDING:

Kumar Patchigolla
Cranfield University
25 PUBLICATIONS **201** CITATIONS

SEE PROFILE

All in-text references underlined in blue are linked to publications on ResearchGate, letting you access and read them immediately.

Available from: Kumar Patchigolla
Retrieved on: 01 February 2016

energy&fuels

Article

pubs.acs.org/EF

Novel Optimized Process for Utilization of CaO-Based Sorbent for Capturing CO_2 and SO_2 Sequentially

Hongwei Chen,[†] Zhenghui Zhao,[†] Xinzhang Huang,[‡] Kumar Patchigolla,[§] Alissa Cotton,[§] and John Oakey*[,§]

[†]Key Laboratory of Condition Monitoring and Control for Power Plant Equipment, North China Electric Power University, Baoding City, Hebei Province, People's Republic of China

[‡]School of Energy and Power Engineering, Shenyang Institute of Engineering, Shenyang City, People's Republic of China

[§]Centre for Energy and Resource Technology (CERT), Cranfield University, United Kingdom

ABSTRACT: Calcium oxide (CaO) based sorbents, used for CO_2 capture in calcination/carbonation cycles, reduce in activity with increasing numbers of cycles, thus reducing the economic benefits of this capture process, generating a significant amount of spent sorbent and raising the potential for pollution from its disposal. This paper presents research into the use of this spent sorbent for the prior capture of sulfur oxides (SO_x), as required when the cycle is used with coal-derived flue gases. Using a thermogravimetric analyzer (TGA), the sulfation behaviors of two limestones from Hebei Province (named LA and LB) were examined after different numbers of calcination/carbonation cycles. The results show that the sulfation conversions for spent sorbent of the LA and LB after 40 cycles were, respectively, about 4% and 14% less than that of the original sorbent, indicating that spent sorbents from CO_2 capture cycles remain active for SO_2 retention. As the number of cycles increased, there was a difference in the sulfation conversions between LA and LB, probably due to the difference in pore structure development for the two limestones as the sulfation reaction progressed. The surface morphology and pore structure of sorbents after different numbers of cycles were examined by scanning electron microscopy (SEM) and nitrogen adsorption/desorption spectroscopy. It was found that the pore size distributions show two peaks in all cases, and as the number of cycles increased, the larger pores fuse together while the number of small pores was not markedly diminished, which is not consistent with the existing sintering model. The observed sintered pore structure provides greater product growing space for reactions to occur in the pore inner surface, which benefits sulfation more than carbonation due to their different product molar volumes, helping to explain why cycled sorbent samples remain active in sulfation.

1. INTRODUCTION

CO_2 emissions, as the main greenhouse gas of concern, are believed to be causing increasingly serious environmental problems, due to global warming effects. As an effective postcombustion technology for capturing CO_2, the cyclic, calcination/carbonation reaction using a CaO-based sorbent has gained increasing focus for its cost effectiveness and flexibility in application to existing power plants.[1−3] However, sorbent activity decays with increasing cycles due to sintering[4] and sulfation,[5] which produce significant amounts of spent sorbent.[6] The spent sorbent is potentially hazardous to the environment due to the presence of unreacted CaO, which can react exothermically when in contact with water to produce $Ca(OH)_2$, which is alkaline and has potential to cause damage to living things.[7,8] The need for the disposal of the spent sorbent may reduce the economic value of the whole process. Considering that SO_2 is also produced from fossil fuel combustion, and can also be captured by the same sorbent, a combination of the two CO_2 and SO_2 capture processes would enhance resource utilization and reduce costs.

Several research studies have shown CaO-based sorbent capturing SO_2 and CO_2 simultaneously, and the results predict that while SO_2 impedes sorbent carbonation, resulting in rapid decay in sorbent activity,[9−11] CO_2 had a beneficial effect on sulfation behavior.[12] This has led to the consideration being given to a new process for utilization of CaO-based sorbents in fluidized bed (FB) systems by separation of the two processes, namely, capturing SO_2 and CO_2 sequentially with a solid CaO-based sorbent. The reaction mechanisms are given in eqs 1 and 2, and the process flow diagram is shown in Figure 1. The flue

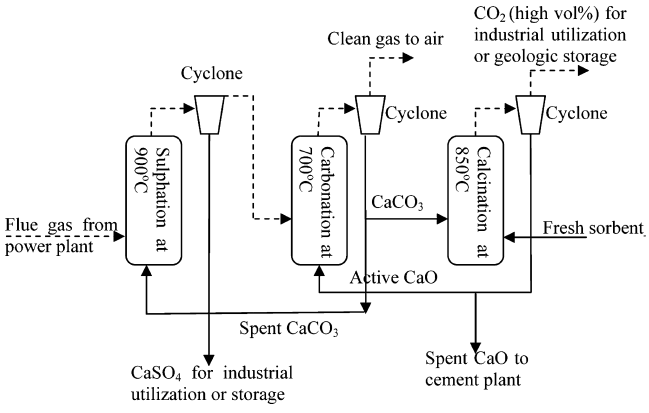

Figure 1. System process of CaO-based sorbent cyclic CO_2 capture preceded by SO_2 retention.

Received: March 21, 2012
Revised: June 24, 2012
Published: July 12, 2012

ACS Publications © 2012 American Chemical Society

dx.doi.org/10.1021/ef300487q | *Energy Fuels* 2012, 26, 5596−5603

gas travels through the desulfurization step before it enters the carbonation reactor. The fresh sorbent is fed directly into the CO_2 capture calcination/carbonation looping cycle, and the spent sorbent is then sent to a separate upstream reactor to perform sulfation. In the ideal case, the sorbent would maintain an acceptable carbonation efficiency for a high number of CO_2 looping cycles, and all spent sorbent would then subsequently be used for desulfurization, resulting in no extra waste being produced when the CO_2 capture process is applied to existing power plants.

$$CaO + CO_2 \Leftrightarrow CaCO_3 \quad \Delta H_{298k} = \mp 178\ kJ/mol \tag{1}$$

$$CaO + SO_2 + \frac{1}{2}O_2 = CaSO_4 \quad \Delta H_{298k} = -502\ kJ/mol \tag{2}$$

Research has been carried out on the single processes of either CO_2 capture or SO_2 retention, and researchers including Anthony et al., 2008, Abanades et al., 2007, and Grace et al., 2007, have identified the reaction mechanisms, sorbent modification, and hydration reactivation processes that take place.[8−19] However, a combination of the two processes is not well addressed in the literature. Sun et al., 2007, showed the influence of carbonation and sulfation when capturing CO_2 and SO_2 sequentially in order to increase the utilization of sorbents.[10,12] At the same time, Manovic et al., 2008, found that spent sorbents that had undergone 10 CO_2 capture cycles had, after steam reactivation, superior characteristics with regard to sulfation.[8,15,20,21] However, hydration may bring another challenge to the process in the form of attrition,[22] and it is not clearly addressed as to why the carbonation and sulfation properties for the same sorbent are different. Further, the sulfation properties of highly cycled sorbents are not reported. To address these challenges, this paper discusses the process of using CaO-based sorbents to capture CO_2 and then to retain SO_2, focusing on the effect of CO_2 looping cycles on SO_2 retention and the microstructural properties of sorbents after several cycles. Further study develops a mechanistic understanding to better describe the reason for the different extents of Ca utilization in carbonation and sulfation for the same sorbent, which may, in turn, provide a possibility for sorbent modification and the reuse of spent sorbent.

2. EXPERIMENTAL SECTION

2.1. Sample and Analysis. The two limestones (labeled LA and LB) used in the experiments were from a quarry in Hebei Province, China. The raw sorbents were crushed and ground first, using a bench-scale ball mill, and then sieved on a vibrating screen to obtain a 38−75 μm diameter size fraction. The compositions as determined by X-ray fluorescence (XRF) elemental analysis are given in Table 1.

Table 1. XRF Elemental Compound Analyses of the Two Limestone Samples

component	LA (wt %)	LB (wt %)	component	LA (wt %)	LB (wt %)
$CaCO_3$	88.7560	93.654	Cr_2O_3	0.0449	0.0495
$MgCO_3$	7.2486	5.1022	SrO	0.0319	0.0734
SiO_2	2.3048	0.7116	MnO	0.0235	0.0734
Al_2O_3	0.7348	0.1915	SO_3	0.0211	0.0139
Fe_2O_3	0.5626	0.1312	P_2O_5		0.0114
K_2O	0.2245	0.0614	total	99.9999	100.074
TiO_2	0.0472				

Two tube furnaces and a thermogravimetric analyzer (TGA) (SMP/PF7548/MET/600W) were used to run the CO_2 looping cycles and sulfation process. A cold field emission scanning electron microscope (SEM) (JSM-7500) was used to observe the particle surface morphology. Pore surface area (Brunauer−Emmett−Teller (BET)) and pore volume distribution (Barrett−Joyner−Halenda (BJH)) of the calcined samples before and after numbers of different CO_2, looping cycles were determined by the nitrogen adsorption/desorption method with a surface area and pore size analyzer (Beckman Coulter SA 3100, U.S.A.). The experimental setup and procedure is shown in Figure 2.

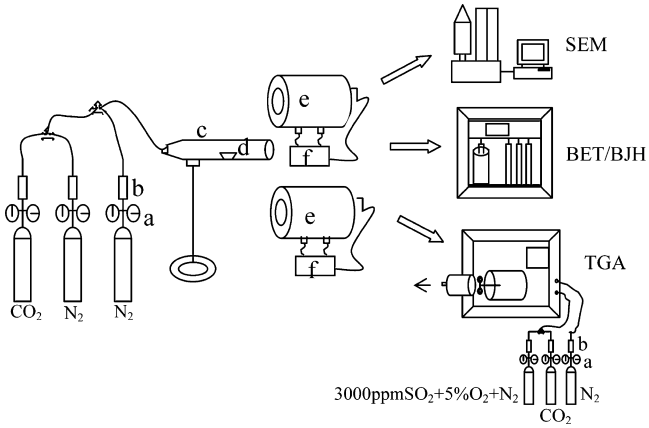

Figure 2. Schematic experimental setup at atmospheric pressure (a, pressure reducing valve; b, flow meter; c, quartz tube; d, quartz plate; e, tube furnace; f, temperature control unit).

2.2. CO_2 Looping Cycles in Tube Furnaces. Two tube furnaces (TF) were used to perform CO_2 looping cycles:[23] one was used as the calciner with a constant temperature of 850 °C and the other was used as the carbonator with a temperature of 700 °C. The limestone samples (~2 g) were suspended on a quartz plate placed in a quartz tube, which could be moved between the two furnaces. The simulated gases, controlled by flow meters, were injected through the quartz tube and maintained the reaction atmosphere, thus protecting samples from contact with air when being moved between furnaces. Calcination was performed under a nitrogen atmosphere (600 mL/min) and carbonation under a gas mixture (600 mL/min) containing 20% CO_2 (N_2 balance). The complete reaction time for both calcination and carbonation was 15 min.[24] The TF samples were subsequently analyzed to determine their pore surface area, surface morphology, and sulfation potential.

2.3. Sulfation Tests Using Thermogravimetric Analysis. A Mettler Toledo TGA/DTA Star* thermogravimetric analyzer (TGA) was used to perform sulfation. The sorbent mass was chosen so that the amount of CaO in each sulfation experiment was approximately the same, at 6 mg, to avoid the influence of gas diffusion on sorbent conversion. The conversions were calculated on the basis of mass change recorded in the TGA. The gas flow rate, controlled by a flow meter, was 60 mL/min. The first step in each experiment was to heat the sorbent in a nitrogen atmosphere at a rate of 50 °C/min to the desired temperature of 850 °C. Under this condition, the sample was calcined for 5 min, during which CO_2 from $CaCO_3$ decomposition was released. The temperature was then increased to 900 °C at which sulfation was performed for 90 min.[25] The gas mixture used was synthetic flue gas (3000 ppm SO_2, 5% O_2, and N_2 balance).

3. RESULT AND DISCUSSION

The XRF chemical analysis (Table 1) shows that both LA and LB contain a high content of $CaCO_3$ (88.7% and 93.6% for LA and LB, respectively), ensuring high efficiency for CO_2 and SO_2 capture. LA contains a higher content of $MgCO_3$ (7.2%) and other impurities including SiO_2, Al_2O_3 and Fe_2O_3, which caused

dx.doi.org/10.1021/ef300487q | Energy Fuels 2012, 26, 5596−5603

LA to be gray in color. LB was white due to the presence of fewer impurities. LA should have more prominent dolomitic characteristics and better cyclic activity due to it having a higher $MgCO_3$ content.[20] However, the following results identify that LB shows a better performance in cyclic calcination/carbonation. This suggests that not only $MgCO_3$ but also other impurities can have an important influence on sorbent activity.

3.1. Pore Surface Area and Volume Analysis. Table 2 shows that both the surface areas and pore volumes of the sorbents decrease as the cycle number increases, particularly during the first few cycles. The reason may be that the surface undulations/roughness that are the main contribution to BET and BJH on the particle surface area, tend to fuse together at high temperatures, and therefore, as the number of cycles increase, larger surface features develops, while the potential for further fusion diminishes.

Table 2. BET Pore Surface Areas and BJH Cumulative Pore Volumes of Samples

	$S_{BET}(m^2/g)$		$V_{BJH}(cm^3/g)$	
no. cycles	LA	LB	LA	LB
0	11.789	15.789	0.148	0.221
7	6.481	6.356	0.029	0.024
15	2.478	4.837	0.018	0.020

The specific pore surface area and pore volume distributions of sorbents were determined using the N_2 adsorption/desorption data. The results are presented in Figures 3 and 4. It can be seen from Figure 3 that pore volume distributions for LA and LB show two peaks in all cases, regardless of the CO_2 looping cycle number. The first peak is in the range 3−6 nm in all samples, while the second peak varied with number of cycles. It is interesting to note that samples analyzed after cycling did not show decreased pore volume in the small pore size range, and even an increase was seen when comparing LA after 7 cycles to 0 cycles, although a decrease was expected as a result of sintering during CO_2 looping cycles. The results were closely matched with those of Manovic et.al,[20] although the sintering model may need further investigation. The second peak is the main contribution to particle pore volume, especially in fresh sorbents. The average pore radius of large pores increased from 50 nm to greater than 100 nm as cycles increased, which coincides with the existing sintering model.[4,26,27] In this pore size range, LA had a lower pore volume than LB in the original samples, but after CO_2 cycling, the pore volume of LA was much higher than that of LB. This means LA was more likely to develop large pores in comparison to LB. Larger pores are beneficial for SO_2 capture, because they are not fully filled after the initial rapid reaction stage, thus further sulfation can occur.

Pore surface area distributions presented in Figure 4 show that a large contribution to surface area was from small pores, and that this contribution decreased with increasing pore radius. In original samples, the contribution from the large pores was obvious, while in samples that experienced CO_2 cycling, this phenomenon disappeared. These results further prove that the CO_2 looping cycles mainly eliminate the large pores rather than the small pores. It is the elimination of larger pores that causes the decline of surface area and sorbent activity.

3.2. Microstructure Analysis, SEM. Surface morphologies of sorbents under different conditions have been analyzed using SEM, and typical microstructures are presented in Figure 5. The same magnification (50 000×) was chosen for all samples such that any size change of prominent features on particle surfaces as cycle numbers increased can be compared directly. From Figure 5a and b, it can be seen that there are many small particles or prominences on the unreacted sample surfaces, which are connected through bridges of about 10 nm in size. It should be noted that a conductive coating (20 nm depth) was added to each sample surface to prevent the accumulation of static electric fields on the specimens during imaging. Considering the thickness of the conductive coat, it is possible to speculate that the real bridges may be about 50 nm in size, which are in accordance with that from BJH models. Another point, which should not be overlooked, was that only the large pores can be seen in the SEM images at the magnification used, while the small pores are very important for carbonation and sulfation. Surface morphologies of samples after seven CO_2 looping cycles are shown in Figure 5c and d, and it can be seen clearly that the prominences disappear and flake-shaped grains are formed on the particle surface. The boundary lines are clear for LA, but they are unclear for LB. There are some deep and disconnected pores among the flake-shaped grains for LA, which are indistinct in LB. After 15 CO_2 looping cycles (Figure 5e and f), the boundary lines are completely lost in both LA and LB. The pores on the surface of LA become larger, while

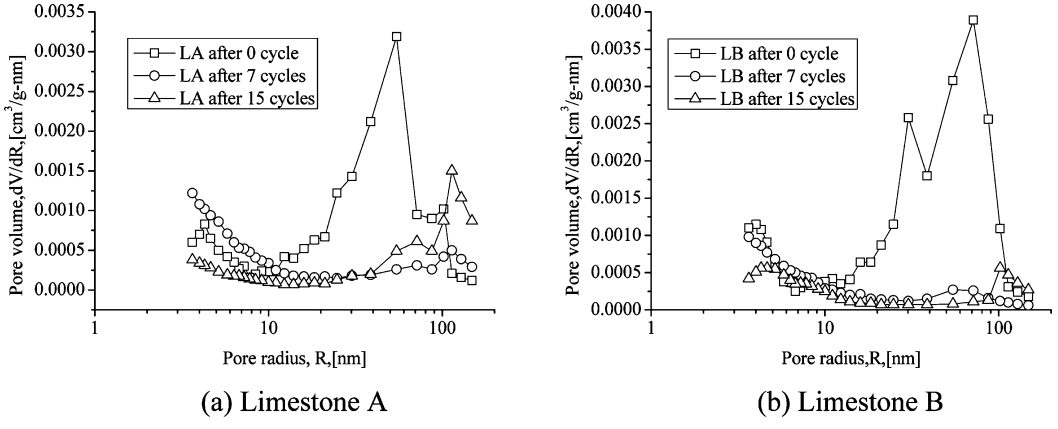

(a) Limestone A (b) Limestone B

Figure 3. BJH pore volume distributions in samples after different CO_2 capture cycles. (Calcination: T_{cal} = 850 °C, gas = pure N_2. Carbonation: T_{car} = 700 °C, gas = 20% CO_2 + N_2 balance.)

dx.doi.org/10.1021/ef300487q | Energy Fuels 2012, 26, 5596−5603

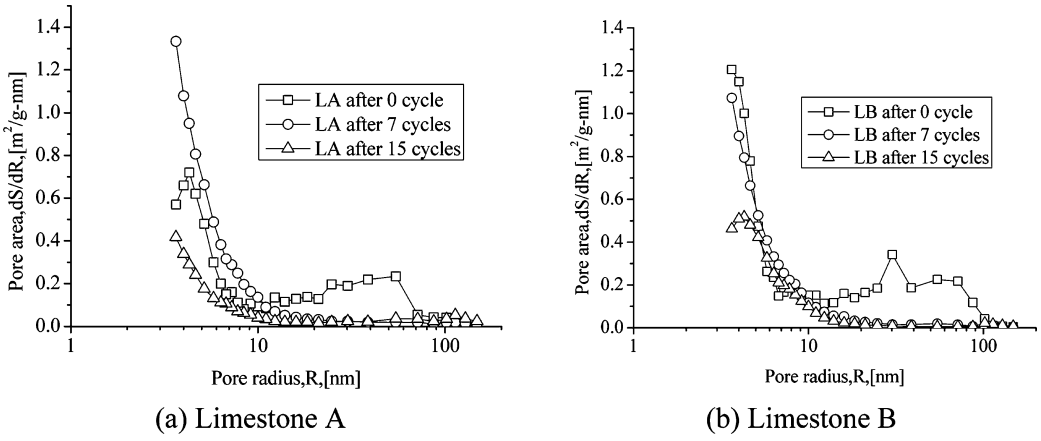

Figure 4. BJH pore surface area distributions in samples after different CO_2 capture cycles. (Calcination: T_{cal} = 850 °C, gas = pure N_2. Carbonation: T_{car} = 700 °C, gas = 20% CO_2 + N_2 balance.)

no pores can be seen for LB, at least within the SEM images. These comparisons between LA and LB suggest that LB is more likely to sinter, given that it has a lower MgO content, known for its antisintering effect.[4]

Parts g and h of Figure 5 show the morphologies of LA and LB after 15 calcination/carbonation cycles followed by sulfation for 60 and 90 min, respectively. Compared with images for unsulfated samples, it can be concluded that the outer covering is composed of $CaSO_4$ crystals. The uneven distribution of the covering for LA may be due to insufficient sulfation time, or the covering has fallen off during processing. There are many cracks present in the product layer, which provide channels for SO_2 diffusion for further sulfation. The formation process of cracks in the product layer can be explained as follows: Growth of the sulfation product is limited by space on the reaction surface, causing new product to push apart the unreacted core and old product. When the reaction driving force outweighs the push force, the reaction continues, and the push force causes the sulfation product to crack, generating more space for new product growth. When the product layer reaches a certain thickness, the push force, which is determined by the reaction driving force, is not enough to crack the old product, so the reaction stops. Sulfation products with cracks easily fall off and may be related to particle attrition.

3.3. Effects of Carbonation Cycles on Sulfation. The CO_2 looping cycles were performed in a tube furnace, and the subsamples were loaded into sealed containers for the next experiments. The conversion of carbonation and sulfation was calculated using the following formulas:

$$X_{car} = \frac{m_{car} - m_{cal}}{M_{CO_2}} \Big/ \frac{m_{start} b}{M_{CaCO_3}} \quad (3)$$

$$X_{sul} = \frac{m_{sul} - m_{cal}}{M_{SO_3}} \Big/ \frac{m_{start} b}{M_{CaCO_3}} \quad (4)$$

where X_{car} denotes the carbonation conversion of sorbent carbonated for 5 min and X_{sul} denotes the sulfation conversion of sorbent sulfated for 90 min; M_{CO_2}, M_{CaCO_3}, M_{SO_3} are the molar masses of CO_2, $CaCO_3$, SO_3, respectively (g/mol); b is the content of $CaCO_3$ in the initial sorbent (% wt); m_{start}, m_{car}, m_{cal} m_{sul} represent sample mass at different stages, namely initial sample, after carbonation, after calcination, and after sulfation, respectively.

As shown in Figure 6, carbonation conversions of both LA and LB decreased with increasing numbers of cycles, especially noticeable for the first seven cycles. LB showed slightly better cycle activity than LA, which is consistent with the analysis in the previous section of this paper that LB is more likely to sinter. It is known that LB has a lower MgO content and thus should be more likely to sinter (as supported by SEM images), but from BET and BJH analysis, it is also known that this phenomenon only occurred in large pores. The small pores that provide a greater contribution to particle total surface area, especially in samples that have undergone CO_2 looping cycles, did not diminish markedly with increasing cycles. The surface area of LB is larger than that of LA, and thus, LB has better cyclic activity durability.

Sulfation was performed in a TGA, and the results presented in Figure 7 illustrate the sulfation levels of sorbents that have undergone different numbers of CO_2 looping cycles. It is interesting that samples analyzed after having undergone several CO_2 looping cycles have only a slightly lower activity with respect to SO_2 capture than the original samples. The carbonation conversion for both original samples (LA and LB) is about 70%, while the sulfation level is only 50% after 90 min. This can be explained by the different molar volumes of $CaCO_3$ (37 cm^3/mol) and $CaSO_4$ (46 cm^3/mol). Both reactions form an outer shell[28−30] on the particle surface, which hinders contact between the reactants (gas and solid). It is more difficult for SO_2 to penetrate the $CaSO_4$ product layer in comparison to CO_2 penetrating the $CaCO_3$ product layer, at the same Ca-utilization level. As cycle numbers increase to seven, the activities for SO_2 capture and CO_2 capture fall to the same value of 40% for both LA and LB. What was more unexpected for LA, was that the sulfation level increased as cycle numbers increased, reaching a peak value of 47.7% after about 15 cycles, close to that of the original sample (48.0%). After this, the value falls again slightly and stabilizes at about 44% after 20 cycles. However, no obvious fluctuation was observed in the graph for LB. Although LB shows superior performance in SO_2 capture compared to LA in fresh sorbents, after seven CO_2 cycles, LB gives a lower sulfation level (about 40%). After 40 CO_2 looping cycles, the ability for further CO_2 capture with two limestones was about 20%, while that for SO_2 retention was above 40%. This means that spent CaO-based sorbents from CO_2 capture should not be discarded but can be reused for SO_2 retention.

dx.doi.org/10.1021/ef300487q | Energy Fuels 2012, 26, 5596−5603

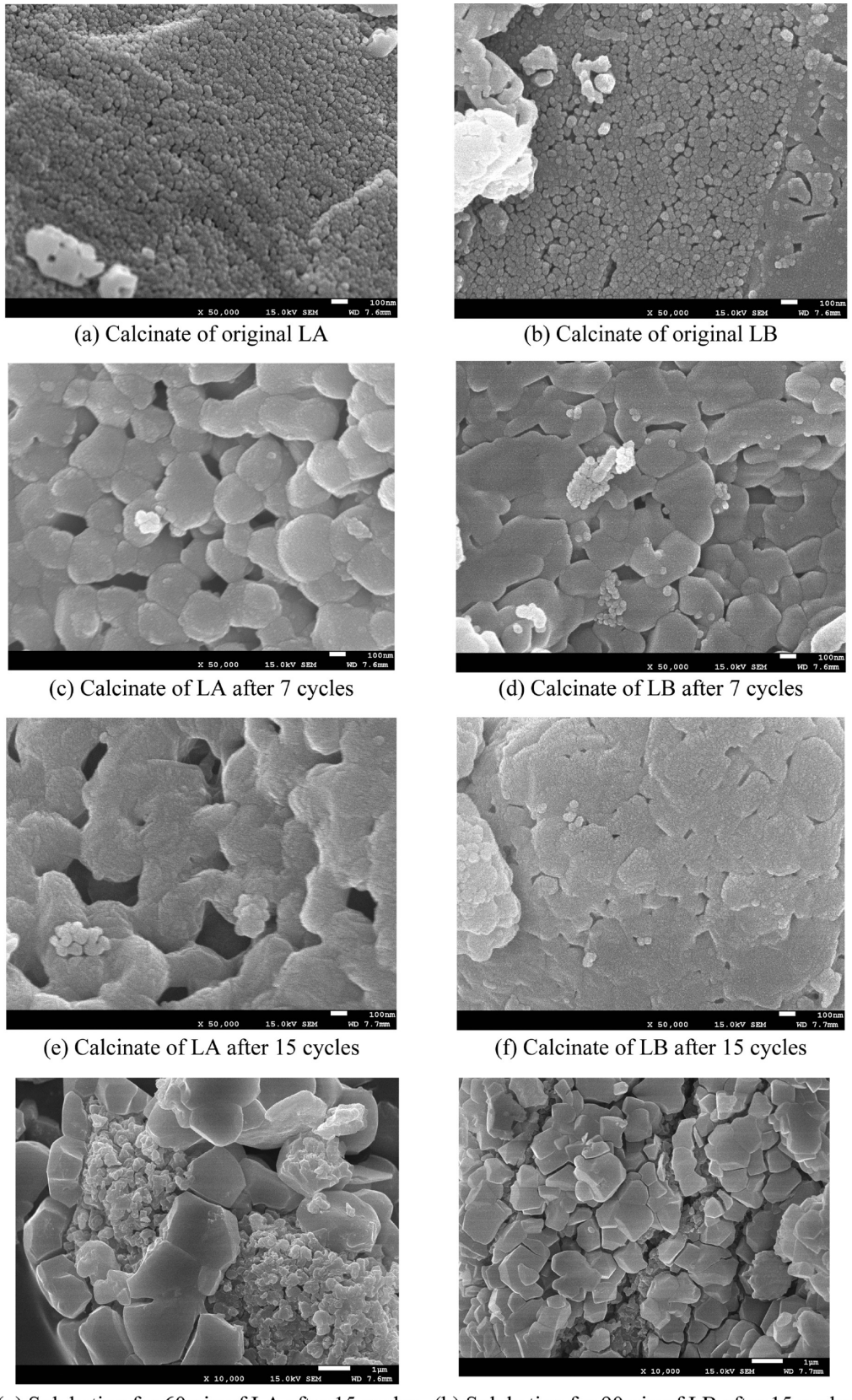

Figure 5. SEM images of particle surface morphologies for two limestones after different numbers of cycles. (Calcination: T_{cal} = 850 °C, gas=pure N_2. Carbonation: T_{car} = 700 °C, gas = 20% CO_2 + N_2 balance. Sulfation: T_{sul} = 900 °C, gas = 3000 ppm +5% O_2 + N_2 balance)

It is well-known that sorbent conversion is mainly controlled by kinetic parameters[31−33] and pore structure.[34] In terms of pore structure, it is known that pore surface area, pore volume, and pore diameter are the major factors influencing Ca-

dx.doi.org/10.1021/ef300487q | Energy Fuels 2012, 26, 5596−5603

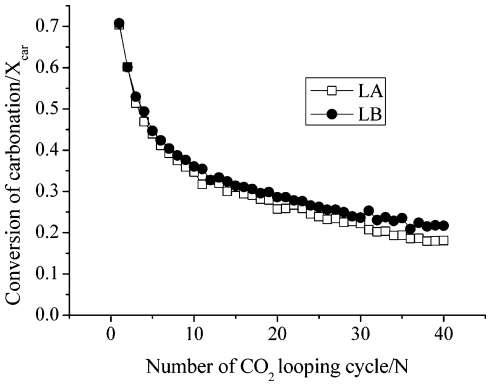

Figure 6. Cyclic carbonation conversion of different limestones. (Calcination: T_{cal} = 850 °C, gas = pure N_2. Carbonation: T_{car} = 700 °C, gas = 20% CO_2 + N_2 balance.)

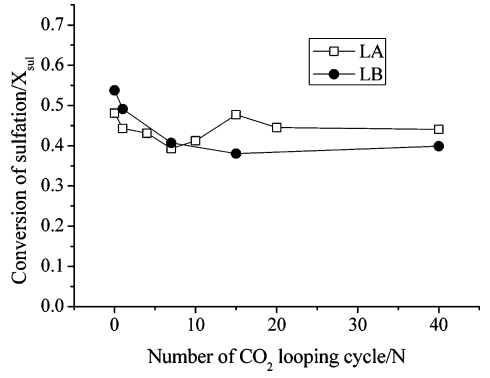

Figure 7. Sulfation conversion for two limestones after different numbers of CO_2 looping cycles. (Calcination: T_{cal} = 850 °C, gas = pure N_2. Carbonation: T_{car} = 700 °C, gas = 20% CO_2 + N_2 balance. Sulfation: T_{sul} = 900 °C, gas = 3000 ppm + 5%O_2 + N_2 balance.)

utilization. Pore surface area represents the field where reactions can take place, while pore volume indicates the space in which products can grow. Pore diameter can be defined as the space limitation in a single pore. The whole surface can be divided into two parts: particle outer surface and pore inner surface. On the outer surface, the product can grow freely until the product layer reaches a critical thickness and the reaction is then controlled by gas diffusion.[35] However, on the inner surface, if the pore diameter is less than 2× critical product thickness, the reaction ceases when the pore is filled by product, but if the pore diameter is greater than 2× critical thickness, the reaction is not limited by space. Unfortunately, it is difficult to measure or calculate the critical product layer thickness, and thus, no agreement has been reached in the literature (49 nm[13] or 0.2 μm[28] for $CaCO_3$ layer, while no exact value was found for $CaSO_4$).

The different capacities for CO_2 capture and SO_2 retention by the two limestones, as shown in Figures 6 and 7, can be viewed as the result of the interaction of pore volume limitations and pore surface area limitations. In the group of small pores (with size of about 5 nm), both carbonation and sulfation reactions are limited by product growing space, while in the group of large pores (with size of about 50 nm), the space limitation is small for carbonation but is still large for sulfation, due to the larger product molar volume of $CaSO_4$ compared to $CaCO_3$. As the number of cycles increase, the decay in activity is mainly due to changes in large pores. In the first seven cycles, the large pores fuse together and form some new pores of an even larger size, which results in a dramatic decline in overall pore surface area and pore volume. Although the Ca-utilization on the inner surface of the new pores is much higher than that on old ones due to larger product growing space being available, the negative effect of surface area loss outweighs the positive effect of space increase, and thus, both carbonation and sulfation conversions decrease. It should be noted that the larger product growing space means that when the pore diameter becomes larger, it can provide a larger space for product growth in a single pore, whereas the overall particle pore volume of sorbent actually decreases due to the elimination of large pores. As the number of cycles further increases ($7 < N < 15$), some large and deep pores can be seen in LA, while fewer pores are visible in LB from SEM images, providing the reason for the different sulfation levels between LA and LB. As the pore diameter enlarges further in LA, the positive effect of space increase on sulfation outweighs the negative effect of surface area loss, and thus, the sulfation level increases. After multiple cycles, the sulfation levels of LB decreased further because the particle surface area decreased and few new pores were formed. When cycle numbers were above 15, the pore diameter in LA exceeds 2× critical thickness and its further increase has no impact on reactions, and thus, the conversion declines again. This analysis also explains the phenomenon that the sulfation level is not directly proportional to sorbent surface area.[36]

The typical sulfation curves of the two limestones from TGA experiments are shown in Figure 8. It can be seen that the

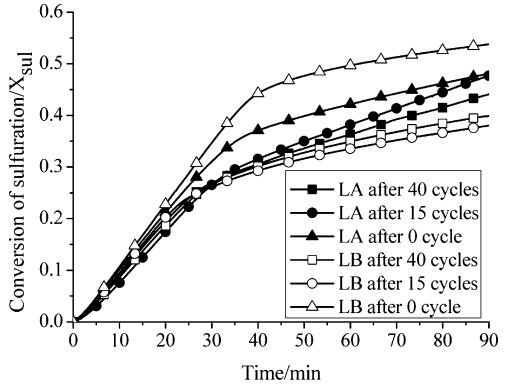

Figure 8. Cyclic sulfation kinetics for two different limestones. (Calcination: T_{cal} = 850 °C, gas = pure N_2. Carbonation: T_{car} = 700 °C, gas = 20% CO_2 + N_2 balance. Sulfation: T_{sul} = 900 °C, gas = 3000 ppm + 5%O_2 + N_2 balance.)

original samples (LA after 0 cycles and LB after 0 cycles) showed the best performance for sulfation. However, in the experiments conducted by Manovic et al.,[20] the sulfation level of samples after 10 cycles was 5% higher than that of original samples. This variance may result from the difference in particle size used in the present work compared with that of Manovic (38−75 μm vs 250−425 μm). It is known that large particles show better resistance to sintering and that more surface area can be created by crushing during process cycles, which is beneficial to reaction rates. Another characteristic of the curves is that the time of the first reaction stage (controlled by kinetics) for all samples that underwent multiple cycles was similar (about 30 min) but much shorter than that for original samples (~37 min for LA and 40 min for LB). Hence, the

dx.doi.org/10.1021/ef300487q | Energy Fuels 2012, 26, 5596−5603

conversion of cycled samples was lower than that of original samples at the end of the first stage. However, with a smaller surface area and larger pores, reaction of the cycled samples became less limited by product growing space than was the case with the original samples. As a result, sulfation of cycled samples in the later stage of reaction (controlled by diffusion) was faster, making a greater contribution to the sulfation level. This phenomenon was more obvious in LA than LB, and was the reason for the different final sulfation levels between LA and LB. Analysis of SEM images shown in Figure 5, identified that many macropores were formed in LA during cycles, while few formed in LB. Reactions continued in the macropores which were not totally filled by products after the first reaction stage. This means that the area where reactions can take place for LA was larger than that for LB, and thus, the reaction rate for LA during the diffusion-controlled stage was faster than that for LB.

In the ideal case for a real power plant system, the production rate of spent sorbent from CO_2 capture should equal the supply rate of the sorbent for SO_2 retention. However, the molar ratio of C to S is very high in coal, meaning that the sorbent needs to maintain an acceptable level of carbonation activity for a higher number of CO_2 capture cycles, compared to the number of cycles required from the same sorbent for SO_2 retention. Taking a typical Chinese anthracite coal[37] as an example, the molar ratio of C/S is 90, so assuming the sorbent activity for CO_2 and SO_2 capture is the same, in order to maintain the production rate of spent sorbent from CO_2 capture equal to the supply rate required for SO_2 retention, the sorbent should experience a minimum of 90 CO_2 capture cycles. From the results presented, the mean carbonation conversions during 40 cycles were 30% and 32% for LA and LB respectively, while the sulfation conversion for sorbents after 40 cycles were 44% and 40% for LA and LB, respectively, meaning that the mean carbonation conversion for a large number of cycles was much lower than the final sulfation conversion. In order to realize the use of the same amount of sorbent to capture all CO_2 and SO_2 from coal, the sorbent should experience a even higher number of cycles than the C:S molar ratio. Low mean carbonation conversion is also a limiting factor in this process; thus, further research is required regarding the enhancement and maintenance of sorbent activity.

4. CONCLUSIONS

Investigation of the sulfation properties of sorbents after varying numbers of CO_2 capture looping cycles was performed in order to examine the influence of carbonation on sulfation, and whether the spent CaO-based sorbents following carbonation still remain active for SO_2 capture. The experimental results show that after 40 CO_2 looping cycles, the CaO-based sorbents are spent with regard to further CO_2 capture, with only about 20% utilization remaining. However, the sorbent remains active with regard to SO_2 retention, with over 40% utilization, a value only slightly lower than that of original limestone samples. This behavior supports the idea that spent CaO-based sorbents from CO_2 looping capture cycles can be used for upstream FB SO_2 retention, thus enhancing resource utilization and reducing the cost of the CO_2 capture process.

From the BET and BJH pore characterization, it was found that the sintering model is only applicable for pores of a large size, while the size change of small pores due to sintering is not obvious in these experiments. Reactions were limited by pore surface area, pore volume, and pore distribution. As the molar volume of $CaCO_3$ is less than that of $CaSO_4$, the sulfation reaction benefits to a greater extent from the increase in pore size than the carbonation reaction does, thus carbonation and sulfation show different activity decay rates for the same sorbent material.

In a real power plant system, to successfully apply this process and avoid producing excess spent sorbent, the sorbent should experience a high number of CO_2 capture cycles before use in SO_2 retention, due to the high molar ratio of C to S in coal. Further research into the enhancement and maintenance of sorbent carbonation for extended numbers of cycles is required.

AUTHOR INFORMATION

Corresponding Author

*E-mail: j.e.oakey@cranfield.ac.uk.

Notes

The authors declare no competing financial interest.

ACKNOWLEDGMENTS

This project is supported by The National Nature Science Foundation (China) (No. 50876030).

REFERENCES

(1) Gupta, H.; Fan, L. S. Carbonation−calcination cycle using high reactivity calcium oxide for carbon dioxide separation from flue gas. *Ind. Eng. Chem. Res.* **2002**, *41*, 4035−4042.

(2) Dean, C. C.; Blamey, J.; Florin, N. H.; Al-Jeboori, M. J.; Fennell, P. S. The calcium looping cycle for CO_2 capture from power generation, cement manufacture and hydrogen production. *Chem. Eng. Res. Des.* **2011**, *89*, 836−855.

(3) Wang, J.; Manovic, V.; Wu, Y.; Anthony, E. J. A study on the activity of CaO-based sorbents for capturing CO2 in clean energy processes. *Appl. Energy* **2010**, *87*, 1453−1458.

(4) Sun, P.; Grace, J. R.; Lim, C. J.; Anthony, E. J. The effect of CaO sintering on cyclic CO_2 capture in energy systems. *AIChE. J.* **2007**, *53*, 2432−2442.

(5) Grasa, G. S.; Alonso, M.; Abanades, J. C. Sulfation of CaO particles in a carbonation/calcination loop to capture CO_2. *Ind. Eng. Chem. Res.* **2008**, *47*, 1630−1635.

(6) Fennell, P. S.; Pacciani, R.; Dennis, J. S.; Davidson, J. F.; Hayhurst, A. N. The effects of repeated cycles of calcination and carbonation on a variety of different limestones, as measured in a hot fluidized bed of sand. *Energy Fuels* **2007**, *21*, 2072−2081.

(7) Abanades, J. C.; Grasa, G.; Alonso, M.; Rodriguez, N.; Anthony, E. J.; Romeo, L. M. Cost structure of a postcombustion CO_2 capture system using CaO. *Environ. Sci. Technol.* **2007**, *41*, 5523−5527.

(8) Manovic, V.; Anthony, E. J.; Lu, D. Y. Sulfation and carbonation properties of hydrated sorbent from a fluidized bed CO_2 looping cycle reactor. *Fuel* **2008**, *87*, 2923−2931.

(9) Ryu, H.; Grace, J. R.; Lim, C. J. Simultaneous CO_2/SO_2 capture characteristics of three limestones in a fluidized-bed reactor. *Energy Fuels* **2006**, *20*, 1621−1628.

(10) Sun, P.; Grace, J. R.; Lim, C. J.; Anthony, E. J. Removal of CO_2 by calcium-based sorbent in the presence of SO_2. *Energy Fuels* **2007**, *21*, 163−170.

(11) Li, Y.; Buchi, S.; Grace, J. R.; Lim, C. J. SO_2 removal and CO_2 capture by limestone resulting from calcination/sulfation/carbonation cycles. *Energy Fuels* **2005**, *19*, 1927−1934.

(12) Sun, P.; Grace, J. R.; Lim, C. J.; Anthony, E. J. Sequential capture of CO_2 and SO_2 in a pressurized TGA simulating FBC conditions. *Environ. Sci. Technol.* **2007**, *41*, 2943−2949.

(13) Alvarez, D.; Abanades, J. C. Determination of the critical product layer thickness in the reaction of CaO with CO_2. *Ind. Eng. Chem. Res.* **2005**, *44*, 5608−5615.
(14) Laursen, K.; Duo, W.; Grace, J. R.; Lim, J. Sulfation and reactivation characteristics of nine limestones. *Fuel* **2000**, *79*, 153−163.
(15) Manovic, V.; Lu, D.; Anthony, E. J. Steam hydration of sorbents from a dual fluidized bed CO_2 looping cycle reactor. *Fuel* **2008**, *87*, 3344−3352.
(16) Grasa, G. S.; Abanades, J. C. CO_2 capture capacity of CaO in long series of carbonation/calcination cycles. *Ind. Eng. Chem. Res.* **2006**, *45*, 8846−8851.
(17) Cao, C.; Zhang, K.; He, C.; Zhao, Y.; Guo, Q. Investigation into a gas−solid−solid three-phase fluidized-bed carbonator to capture CO_2 from combustion flue gas. *Chem. Eng. Sci.* **2011**, *66*, 375−383.
(18) Li, Y.; Zhao, C.; Chen, H.; Liu, Y. Enhancement of Ca-based sorbent multicyclic behavior in Ca looping process for CO_2 separation. *Chem. Eng. Technol.* **2009**, *32*, 548−555.
(19) Chen, H.; Zhao, C.; Li, Y.; Ren, Q. Feasibility of CO_2/SO_2 uptake enhancement of calcined limestone modified with rice husk ash during pressurized carbonation loop. *J. Environ. Manage.* **2012**, *93*, 235−244.
(20) Manovic, V.; Anthony, E. J. Sequential SO_2/CO_2 capture enhanced by steam reactivation of a CaO-based sorbent. *Fuel* **2008**, *87*, 1564−1573.
(21) Manovic, V.; Anthony, E. J. SO_2 retention by reactivated CaO-based sorbent from multiple CO_2 capture cycles. *Environ. Sci. Technol.* **2007**, *41*, 4435−4440.
(22) Chen, Z.; Grace, J. R.; Lim, C. J. Development of particle size distribution during limestone impact attrition. *Powder Technol.* **2011**, *207*, 55−64.
(23) Wang, Y.; Lin, S.; Suzuki, Y. Experimental study on CO_2 capture conditions of a fluidized bed limestone decomposition reactor. *Fuel Process. Technol.* **2010**, *91*, 958−963.
(24) Okunev, A. G.; Nesterenko, S. S.; Lysikov, A. I. Decarbonation rates of cycled CaO absorbents. *Energy Fuels* **2008**, *22*, 1911−1916.
(25) Liu, N.; Cheng, L.; Luo, Z.; Chen, B.; Cen, K. Microstructure and sulfation characteristics of calcium-based sorbents. *CIESC J.* **2004**, *55*, 635−639.
(26) Fierro, V.; Adánez, J.; García-Labiano, F. Effect of pore geometry on the sintering of Ca-based sorbents during calcination at high temperatures. *Fuel* **2004**, *83*, 1733−1742.
(27) Sun, P.; Grace, J. R.; Lim, C. J. The effect of CaO sintering on cyclic CO_2 capture in energy systems. *AIChE J.* **2007**, *53*, 2432−2442.
(28) Manovic, V.; Anthony, E. J. Sintering and formation of a nonporous carbonate shell at the surface of CaO-based sorbent particles during CO_2-capture cycles. *Energy Fuels* **2010**, *24*, 5790−5796.
(29) Duo, W.; Laursen, K.; Lim, J.; Grace, J. Crystallization and fracture: Formation of product layers in sulfation of calcined limestone. *Powder Technol.* **2000**, *111*, 154−167.
(30) Borgwardt, R. H.; Bruce, K. R.; Blake, J. An Investigation of product-layer diffusivity for CaO sulfation. *Ind. Eng. Chem. Res.* **1987**, *26*, 1993−1998.
(31) Li, Y.; Zhao, C. Carbonation characteristics in calcium-sorbents cyclic calcination/carbonation reaction process. *Proc. CSEE* **2008**, *28*, 55−60.
(32) Charitos, A.; Hawthorne, C.; Bidwe, A. R.; Sivalingam, S.; Schuster, A.; Spliethoff, H.; Scheffknecht, G. Parametric investigation of the calcium looping process for CO_2 capture in a 10 kWth dual fluidized bed. *Int. J. Greenhouse Gas Control* **2010**, *4*, 776−784.
(33) Manovic, V.; Anthony, E. J. Parametric study on the CO_2 capture capacity of CaO-based sorbents in looping cycles. *Energy Fuels* **2008**, *22*, 1851−1857.
(34) Alvarez, D.; Abanades, J. C. Pore-size and shape effects on the recarbonation performance of calcium oxide submitted to repeated calcination/recarbonation cycles. *Energy Fuels* **2005**, *19*, 270−278.
(35) Mess, D.; Sarofim, A. F.; Longwell, J. P. Product layer diffusion during the reaction of calcium oxide with carbon dioxide. *Energy Fuels* **1999**, *13*, 999−1005.
(36) Cao, L.; He, R. Effect of CaO pore parameters on desulfurization reaction rates. *J. Tsinghua Univ. (Sci. Technol.)* **2010**, *50*, 283−286.
(37) Wang, C.; Lei, M.; Yan, W.; Wang, S.; Jia, L. Combustion characteristics and ash formation of pulverized coal under pressurized oxy-fuel conditions. *Energy Fuels* **2011**, *25*, 4333−4344.